

<Electronic Supplementary Information>

Insight into systematic formation of hexafluorosilicate during crystallization via self-assembly in glass vessel

Dongwon Kim,^a Jihun Han,^a Ok-Sang Jung,^{*a} and Young-A Lee^{*b}

^aDepartment of Chemistry, Pusan National University, Busan 46241, Republic of Korea

E-mail: oksjung@pusan.ac.kr

^bDepartment of Chemistry, Jeonbuk National University, Jeonju 54896, Republic of Korea

E-mail: ylee@jbnu.ac.kr

Table S1 Crystallographic Data for $[(\text{SiF}_6)_2@\text{Cu}_3\text{L}^1_4](\text{SiF}_6)\cdot 16\text{CH}_3\text{OH}$ and $[(\text{SiF}_6)_2@\text{Zn}_2\text{L}^2_4](\text{SiF}_6)\cdot 2\text{C}_4\text{H}_8\text{O}\cdot 4\text{CH}_2\text{Cl}_2$.

	$[(\text{SiF}_6)_2@\text{Cu}_3\text{L}^1_4](\text{SiF}_6)\cdot 16\text{CH}_3\text{OH}$	$[(\text{SiF}_6)_2@\text{Zn}_2\text{L}^2_4](\text{SiF}_6)\cdot 2\text{C}_4\text{H}_8\text{O}\cdot 4\text{CH}_2\text{Cl}_2$
Formula	$\text{C}_{216}\text{H}_{168}\text{Cu}_3\text{F}_{18}\text{N}_{24}\text{O}_{36}\text{Si}_3$	$\text{C}_{60}\text{H}_{54}\text{Cl}_4\text{F}_6\text{N}_6\text{O}_{13}\text{SiZn}$
M_w	4292.62	1416.35
Cryst. sys.	Monoclinic	Tetragonal
Space group	$C2$	$P4/n$
a (Å)	38.961(8)	20.713(2)
b (Å)	21.921(4)	20.713(2)
c (Å)	23.987(5)	15.855(1)
α (°)	90	90
β (°)	116.69(3)	90
γ (°)	90	90
V (Å ³)	18304(8)	6803(1)
Z	2	4
ρ (g cm ⁻³)	0.779	1.383
μ (mm ⁻¹)	0.281	0.615
F(000)	4422	2904
Independent reflections (R_{int})	32740 (0.0749)	6691 (0.0807)
GooF	0.786	1.037
Absolute structure parameter	0.020(5)	-
Final R indices [$I > 2\sigma(I)$]	$R_1 = 0.0412$, $wR_2 = 0.0906$	$R_1 = 0.0633$, $wR_2 = 0.1956$
R indices (all data)	$R_1 = 0.1158$, $wR_2 = 0.1100$	$R_1 = 0.0963$, $wR_2 = 0.2327$
Largest diff. peak and hole (e/Å ³)	0.224 and -0.244	1.500 and -0.620

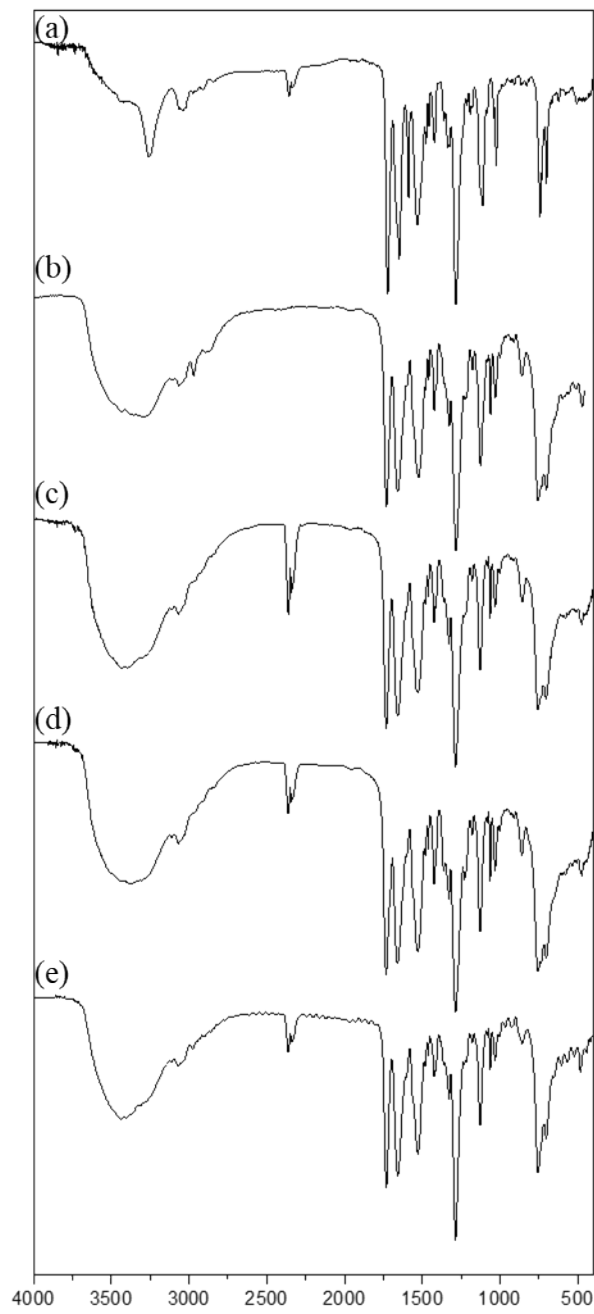


Fig. S1 IR spectra for L¹ (a), [(SiF₆)₂@Cu₃L¹₄](SiF₆)·16CH₃OH using Method 1 (b), [(SiF₆)₂@Cu₃L¹₄](SiF₆)·16CH₃OH using Method 2 (c), [(SiF₆)₂@Cu₃L¹₄](SiF₆)·16CH₃OH using Method 3 (d), and [(SiF₆)₂@Cu₃L¹₄](SiF₆)·16CH₃OH using Method 4 (e).

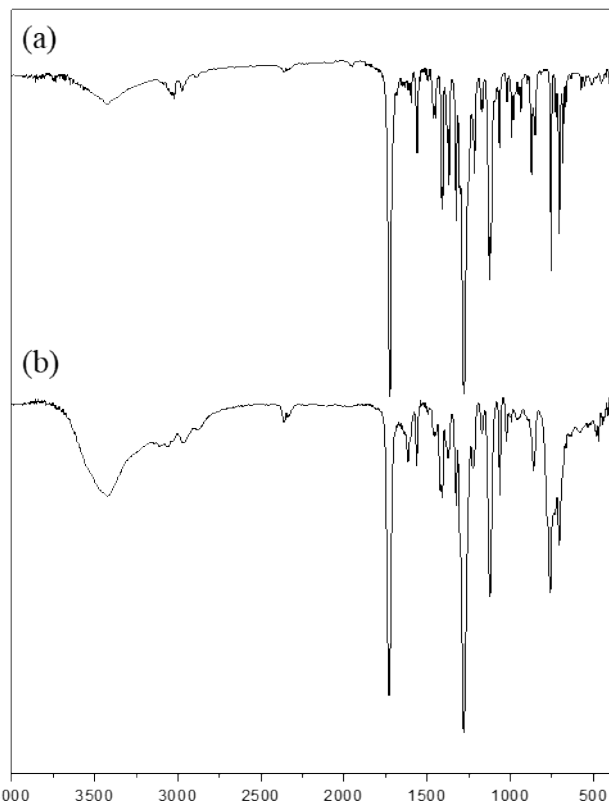


Fig. S2 IR spectra for L² (a), and [(SiF₆)@Zn₂L²₄](SiF₆)·2C₄H₈O·4CH₂Cl₂ (b).

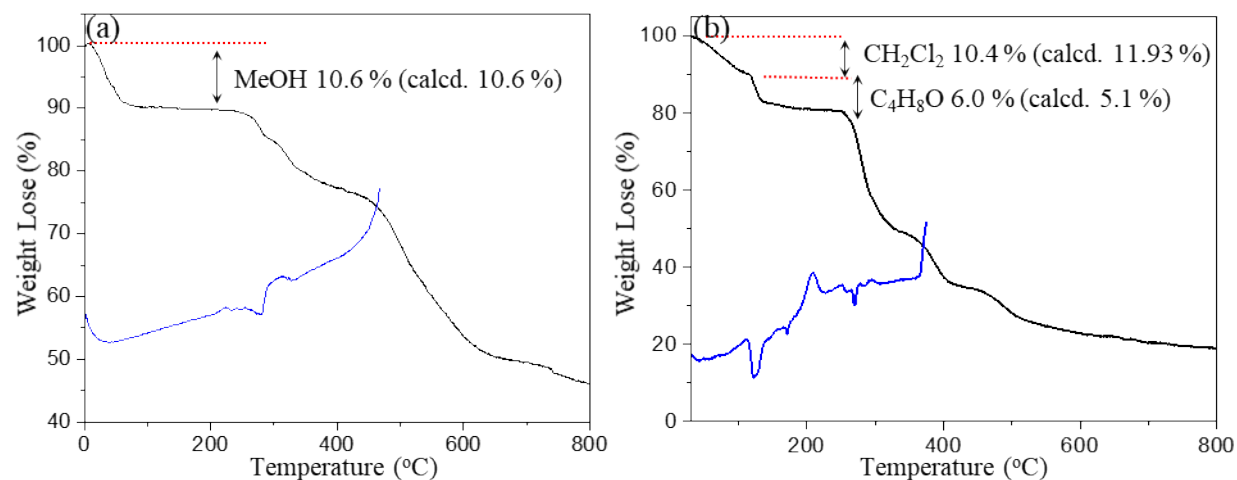


Fig. S3 TG and DSC curves for $[(\text{SiF}_6)_2@\text{Cu}_3\text{L}^4](\text{SiF}_6)\cdot 16\text{CH}_3\text{OH}$ (a), and $[(\text{SiF}_6)_2@\text{Zn}_2\text{L}^4](\text{SiF}_6)\cdot 2\text{C}_4\text{H}_8\text{O}\cdot 4\text{CH}_2\text{Cl}_2$ (b).

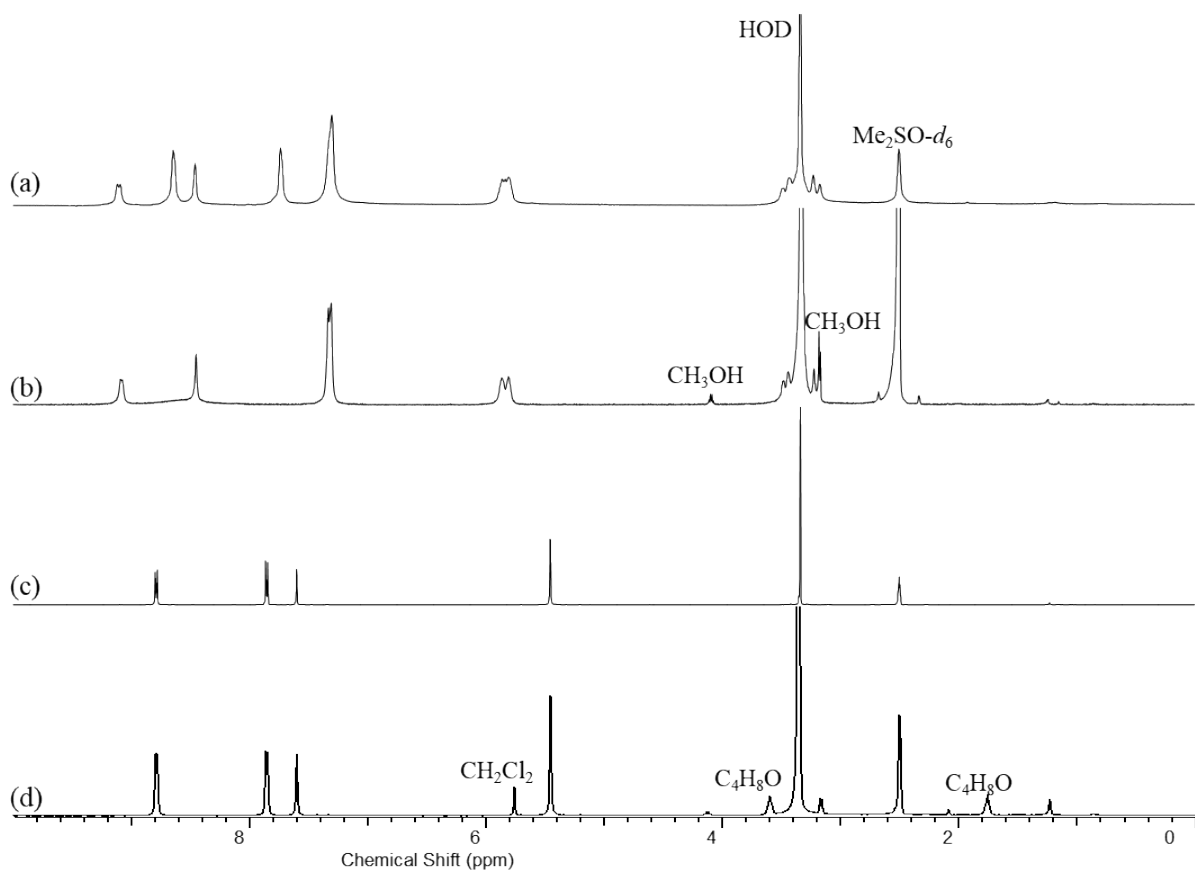


Fig. S4 ^1H NMR spectra for L^1 (a), $[(\text{SiF}_6)_2@\text{Cu}_3\text{L}^1_4](\text{SiF}_6)\cdot 16\text{CH}_3\text{OH}$ (b), for L^2 (c), and $[(\text{SiF}_6)_2@\text{Zn}_2\text{L}^2_4](\text{SiF}_6)\cdot 2\text{C}_4\text{H}_8\text{O}\cdot 4\text{CH}_2\text{Cl}_2$ (d).

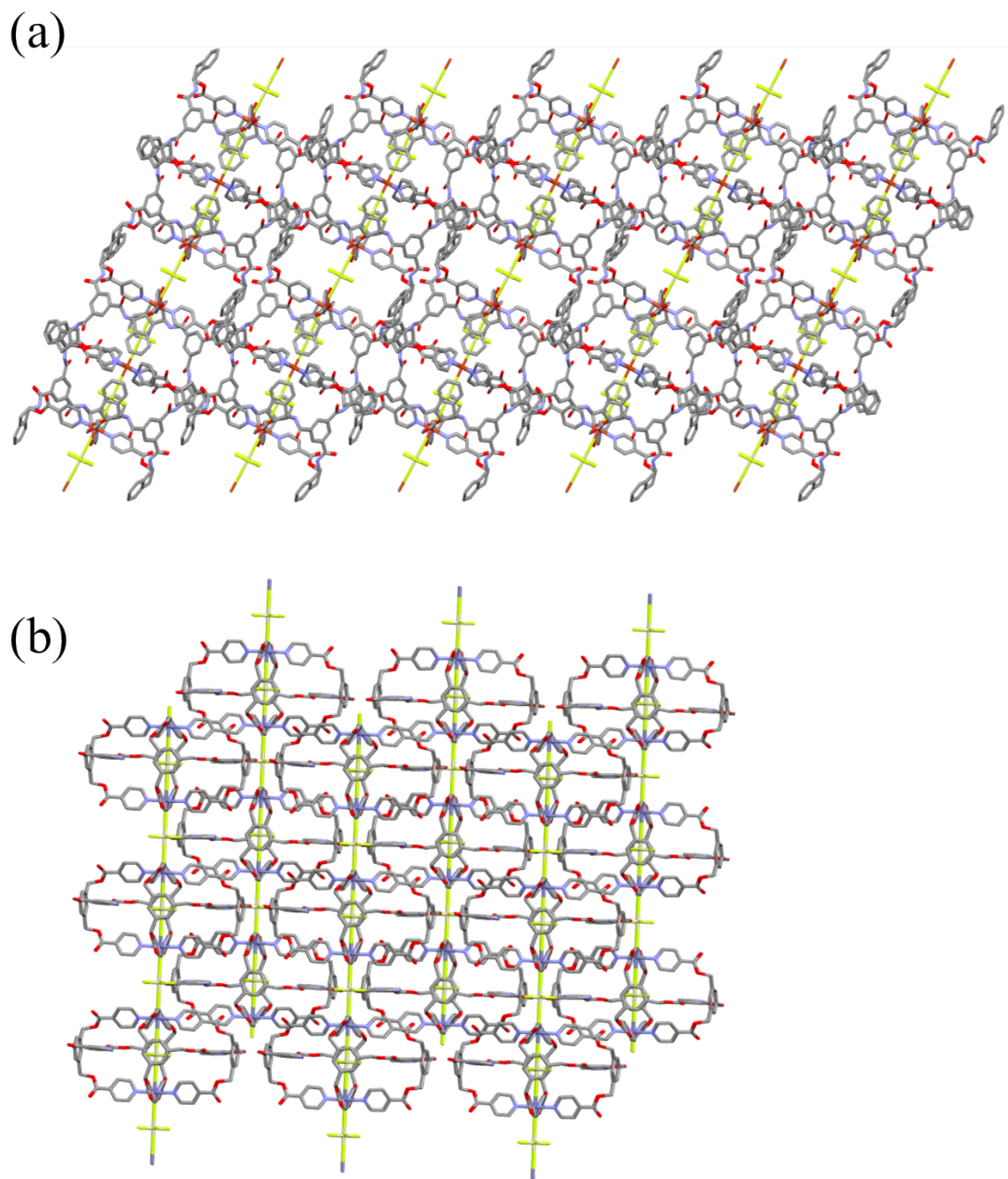


Fig. S5 The packing diagram represent the structure of $[(\text{SiF}_6)_2@\text{Cu}_3\text{L}^4](\text{SiF}_6)\cdot 16\text{CH}_3\text{OH}$ (a), and $[(\text{SiF}_6)_2@\text{Zn}_2\text{L}^4](\text{SiF}_6)\cdot 2\text{C}_4\text{H}_8\text{O}\cdot 4\text{CH}_2\text{Cl}_2$ (b).

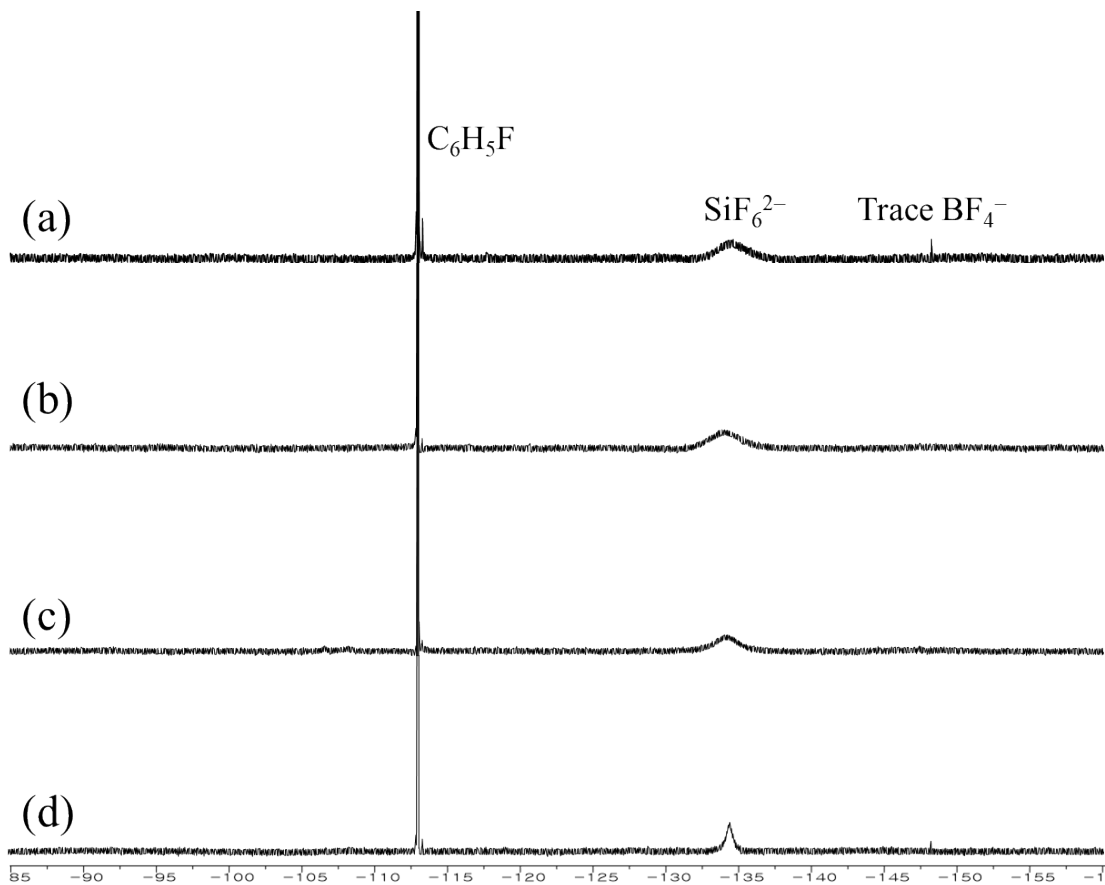


Fig. S6 ^{19}F NMR spectra for $[(\text{SiF}_6)_2@\text{Cu}_3\text{L}^1_4](\text{SiF}_6)\cdot 16\text{CH}_3\text{OH}$ using *Method 1* (a), $[(\text{SiF}_6)_2@\text{Cu}_3\text{L}^1_4](\text{SiF}_6)\cdot 16\text{CH}_3\text{OH}$ using *Method 2* (b), $[(\text{SiF}_6)_2@\text{Cu}_3\text{L}^1_4](\text{SiF}_6)\cdot 16\text{CH}_3\text{OH}$ using *Method 3* (c), and $[(\text{SiF}_6)_2@\text{Zn}_2\text{L}^2_4](\text{SiF}_6)\cdot 2\text{C}_4\text{H}_8\text{O}\cdot 4\text{CH}_2\text{Cl}_2$ (d). The chemical shifts were measured relative to a $\text{C}_6\text{H}_5\text{F}$ internal standard.